



# TRANSLATIONAL CHEMISTRY

AN INTERFACE JOURNAL

[HTTPS://WWW.TRANSLATIONALCHEMISTRY.COM/](https://www.translationalchemistry.com/)



ORIGINAL ARTICLE | DOI: 10.5584/translationalchemistry.v1i1.239

## Increasing the potential of enzymatic environmental reactions by applying Tesla valve

Agnieszka Rybarczyk<sup>1,\*</sup>, Malwina Nowak<sup>1</sup>, Patrycja Frąckowiak<sup>1</sup>, Adam Grzywaczyk<sup>1</sup>, Wojciech Smulek<sup>1</sup>, Jakub Zdarta<sup>1,\*</sup>

<sup>1</sup>Institute of Chemical Technology and Engineering, Faculty of Chemical Technology, Poznan University of Technology, Berdychowo 4, PL-60965 Poznan, Poland

Received: April 2025 Accepted: May 2025 Available Online: June 2025

### ABSTRACT

The Tesla valve has been investigated as a potential bioreactor for enzymatic reactions. The reactor obtained through 3D printing was optimized in a colorimetric neutralization reaction of sodium hydroxide with hydrochloric acid and was tested for its ability to facilitate the enzymatic degradation of 17 $\alpha$ -ethynylestradiol (EE2) using laccase. Our study demonstrates the feasibility of utilizing Tesla valves as efficient and cost-effective enzymatic bioreactors for the degradation of pharmaceutical pollutants. The Tesla reactor enables high EE2 degradation efficiency (up to 84%) under optimal flow conditions, offering a sustainable alternative for environmental remediation processes. An additional advantage of using the Tesla valve is its simple design, the absence of mechanical stirrers, and its ability to prevent backflow, contributing to lower operational costs and increased durability. All these findings suggest a high potential for the application of the Tesla valve as a bioreactor in enzymatic processes.

**Keywords:** Tesla valve, bioreactors, 3D printing, enzymatic reactions, EE2 degradation

### Introduction

Modern biocatalysis based on enzyme engineering aimed at improving industrial processes. Enzymes, as efficient and selective catalysts, offer more favorable working conditions in terms of energy efficiency and environmental impact compared to traditional chemical catalysts. Enzyme-catalyzed chemical reactions are not limited to those occurring naturally, enabling new research on the degradation of persistent pollutants and polymers, as well as atom-efficient synthesis of complex biomolecules [1]. Such enzymes include oxidoreductases – biocatalysts that catalyze redox reactions. Due to their wide substrate diversity, they can be applied in various biocatalytic processes through homogeneous and heterogeneous catalysis [2].

Due to the increasing interest in enzymatic processes, a growing number of studies focus on designing these processes and optimizing the selection of reactors has appeared. The choice of the appropriate type of operation carried out in reactors significantly affects reaction efficiency, enzyme stability, and overall process performance [3, 4]. Currently, many different types of biocatalytic reactors are in use. This diversity results from the growing number of enzyme-based processes and modern engineering solutions.

Reactors, depending on their mode of operation and design, can be classified into batch reactors, flow reactors, membrane reactors, and fluidized bed reactors [5]. In a batch reactor, all reagents, including the enzyme and substrate, are loaded into the reactor at the beginning of the process. The reaction proceeds without the addition of fresh substrate or removal of the product until the desired conversion is achieved. Batch reactors are most used in processes involving enzymes in solutions, although immobilized enzymes can also be effectively applied. Typically, the biocatalyst in the form of particles is evenly dispersed in the substrate solution, and mechanical stirrers ensure proper mixing. Batch processes usually require long reaction times [6]. Rather, batch reactors are widely used for producing various products in the chemical and biotechnological industries. Consequently, in recent years, there has been growing interest in optimizing process parameters to maximize economic profit, improve conversion rates, or minimize reaction time [7]. A batch reactor is particularly suitable for products such as pharmaceuticals, polymers, biotechnological products, or other chemical compounds [8].

The use of continuous-flow biochemical reactors is gaining importance in the production of specialty chemicals, pharmaceuticals, biotherapeutics, and biofuels. They also have great

\*Corresponding author: Agnieszka Rybarczyk (agnieszka.rybarczyk@doctorate.put.poznan.pl); Jakub Zdarta (jakub.zdarta@put.poznan.pl)

potential for bioanalytical applications [9]. In a flow reactor, substrates are continuously supplied, and products are continuously removed. This type of apparatus operates mainly under steady-state conditions. A key characteristic of a flow reactor is that all reaction parameters depend on the position within the apparatus rather than the reaction time. This type of reactor is used in processes requiring high production efficiency, particularly for fast reactions. Note also that both free and immobilized enzymes can be used in flow reactors [10, 5].

An enzymatic membrane reactor (EMR) is considered a unique apparatus that can simultaneously facilitate both catalytic reactions and product separation, particularly in the hydrolysis of large molecules that enables more cost-effective processes [11]. Membrane reactors integrate membrane separation processes with chemical or biochemical reactions within a single unit. This combination provides higher conversion, improved selectivity, and a compact, cost-efficient reactor design [12]. Membranes in such reactors can be classified into two types: active and passive membranes. In an active membrane, biocatalysts are immobilized, and as substrates pass through their pores, an enzyme-catalyzed reaction occurs. In contrast, a passive membrane functions as a filter that, through appropriate pore size selection, acts as a barrier for catalysts and substrates while allowing only reaction products and solvents to pass through. This system ensures complete separation of substrates and products during the process [5].

A commonly used type of enzymatic reactor is also the fluidized bed reactor (FBR), which can operate continuously. Compared to packed-bed and stirred-tank reactors, fluidized bed reactors are more suitable when substrates are viscous or particulate, as they result in lower pressure losses and a more uniform flow distribution [13-15]. A FBR is a variation of a batch reactor that operates exclusively in an upward-flow mode. The substrate solution is fed from the bottom of the bed at a velocity sufficient to suspend particles, while the pressure drop of the flowing fluid effectively supports the bed's weight. Fluidization can be achieved using either liquids or gases. The main advantage of using a fluidized bed bioreactor is the large specific surface area of the fine-grained packing material. Immobilizing enzymes on the packing particles further separates the residence times of biomass and liquid in the reactor, preventing catalyst washout. This allows for feeding the reactor with a substrate stream at a higher flow rate [8].

In response to the growing demand for more efficient and compact biocatalytic systems, increasing efforts are being made to develop alternative types of reactors. Among them, the Tesla valve stands out as a particularly promising solution. Unlike traditional reactors

that rely on mechanical components or complex flow regulation systems, the Tesla valve enables preferential fluid flow in one direction without the use of moving parts. This unique feature simplifies both the design and operation of the reactor, making it a highly suitable option for continuous-flow enzymatic processes. Integrating biocatalysts within or along the Tesla valve's channels allows for the creation of a compact enzymatic reactor capable of efficiently treating wastewater contaminated with pharmaceutical compounds. In this context, the Tesla valve may offer new perspectives by overcoming many limitations of conventional reactors. Based on these advantages, the present study aimed to utilize and optimize the Tesla valve as an enzymatic reactor for the removal of pharmaceutical pollutants from water streams. The influence of various process parameters on reaction rate and reactor performance was thoroughly investigated and supported by computational modeling to achieve the highest possible removal efficiency.

## Material and Methods

### Materials and reagents

Sodium hydroxide (98%), hydrochloric acid (37%), bromothymol blue (3',3''-dibromothymolsulfonphthalein), laccase from *Trametes versicolor* (EC 1.10.3.2), and 17 $\alpha$ -ethinyloestradiol (EE2) were received from Sigma-Aldrich. 50 mM acetate buffer pH 5 was freshly prepared.

### Reactor fabrication

A model of a flow reactor with a Tesla microvalve was designed using Fusion 360 (Autodesk Inc., USA) and prepared for 3D printing in PrusaSlicer software (Prusa, Czech Republic) using Fused Deposition Modelling technology. The set process parameters are summarised in **Table 1**. Printing was carried out on a Prusa I3 MK3 printer (Prusa, Czech Republic) equipped with a 0.4 mm nozzle, using polylactide (PLA) filaments in white and transparent (Spectrum Filaments, Poland).

### Hydrodynamic calculations

In order to determine the dependence of the Reynolds number on the flow rate of the reactant streams, hydrodynamic calculations were made to determine the volumetric flow rate ( $V'$ ), the averaged flow rate ( $v$ ), and the apparent flow rate ( $u$ ), which in turn allowed

**Table 1** | Summary of the settings used in the reactor printing.

Parameter	Value
Layer height (mm)	0.1
Filling density (%)	50.0
Nozzle temperature (°C)	208.0
Table temperature (°C)	60.0
Retraction (mm)	2.0
Z-hop (mm)	0.4

the calculation of the averaged ( $Re_v$ ) and apparent ( $Re_u$ ) Reynolds number. Calculations were made using equations (1-5):

$$(1) \quad V' = \frac{V_r}{t} \cdot (\text{mL/s})$$

Where:  $V_r$  - volume of the reactor (mL), while  $t$  - time for the liquid to flow through the reactor (s).

$$(2) \quad v = \frac{l}{t} \text{ (m/s)}$$

Where:  $l$  - total length of flow channels (m), and  $t$  - time of fluid flow through the reactor (s).

$$(3) \quad u = \frac{L}{t} \text{ (m/s)}$$

Where:  $L$  - length of the reactor (m), while  $t$  - time for the liquid to flow through the reactor (s).

$$(4) \quad Re_v = \frac{\rho \cdot v \cdot d}{\eta} \text{ (-)}$$

Where:  $\rho$  - density of water at 25 °C (kg/m<sup>3</sup>),  $v$  - averaged flow rate (m/s),  $d$  - reactor flow diameter (m), and  $\eta$  - water viscosity at 25 °C (Pa\*s).

$$(5) \quad Re_u = \frac{\rho \cdot u \cdot d}{\eta} \text{ (-)}$$

Where:  $\rho$  - density of water at 25 °C (kg/m<sup>3</sup>)  $u$  - apparent flow rate (m/s),  $d$  - reactor flow diameter (m), and  $\eta$  - water viscosity at 25 °C (Pa\*s).

#### Tesla reactor flow study based on the reaction of sodium hydroxide with hydrochloric acid

A reaction between 0.001 M hydrochloric acid and 0.001 M sodium hydroxide in the presence of bromothymol blue, a universal pH indicator, was carried out to investigate the flow characteristics of the reactant streams in the reactor. Eleven experiments were performed, during which the liquid flow through the reactor was monitored at varying flow rates (1, 2, or 3 mL/min). The selection of flow rates was based on preliminary laboratory tests and an analysis of the literature. The process was carried out for 10 minutes following the emergence of the first drop of the reaction mixture from the reactor. During this period, 10 samples were collected at 1-minute intervals. The relationship between the final solution pH and the flow rate of the reactant streams was assessed by measuring pH at 0, 5, and 10 minutes. The samples were subsequently analyzed using UV-Vis spectroscopy in a Jasco V-750 spectrophotometer (Jasco, Japan) over a wavelength range of 280–800 nm.

#### Study on the degradation of estrogens by free enzymes in a Tesla reactor

The efficiency of enzymatic degradation of estrogens in the Tesla reactor was investigated using a laccase solution (3 mg/mL) and a 17 $\alpha$ -ethynylestradiol solution (0,1 mg/L) prepared in pH 5 acetate buffer. Eleven analogous experiments were conducted at flow rates of 1, 2, or 3 mL/min for each stream, with the residence time of the liquid within the reactor being measured. The reaction proceeded for 10 minutes following the emergence of the first drop of liquid from the reactor, during which 10 samples were collected at 1-minute intervals. The pH of the collected samples was measured at 0, 5, and 10 minutes, followed by analysis via gas chromatography-mass spectrometry (GC-MS). Post-reaction samples were lyophilized using an Alpha 1.4 LD plus lyophilizer (0.36 mbar, -30 °C, 96 h). The resulting residue was resuspended in dimethylformamide (DMF) and transferred to vials. Samples were derivatized by adding N,O-Bis(trimethylsilyl)trifluoroacetamide (BSTFA) with 1% trimethylchlorosilane (TMCS) and subsequently heated at 65 °C for 2 hours. The prepared samples were then subjected to chromatographic analysis. Quantitative analysis of the target compounds was performed using a Pegasus 4D gas chromatograph (Leco, USA) equipped with a BPX-5 column (28 m  $\times$  250  $\mu$ m  $\times$  0.25  $\mu$ m). Helium was employed as the carrier gas. A 1- $\mu$ L sample was injected at 250 °C. The chromatographic separation was conducted under programmed temperature conditions: an initial temperature of 80 °C was maintained for 1 minute, followed by an increase of 20 °C/min to 200 °C, then an increase of 8°C/min to 280 °C, with the final temperature held for 3 minutes. The chromatograph was coupled to a mass spectrometer which analyzed the eluent from the column using an ion source operating in positive ion mode. The temperature of the ion source was 250 °C and the energy was 70 eV. Chroma TOF-GC v4.51.6.0 software was used to analyze the data.

#### Statistical analysis of the results

The results obtained were collated and statistically analyzed using MODDE<sup>®</sup> 12.1 software (Sartorius Stedim Data Analytics, Germany). The analysis was based on the assumption that there were two variables in the experiment performed - the volumetric flow rate of component A and the volumetric flow rate of component B. The responses of the system - the Tesla reactor - on the other hand, were the actual and apparent linear flow velocity (and the Reynolds numbers calculated from them), the pH of the solution at the outlet of the reactor, and the efficiency of the estrogen degradation process. The calculations were performed in post-ANOVA mode based on three independent measurements of each parameter, together with the default values of the analytical parameters suggested by the software developers. The linear model proved to be the most appropriate (compared to the quadratic models tested) and best correlated with the results obtained, maintaining a confidence level of  $p < 0.05$ . For individual parameters, the linear equations were as follows:

$$pH = 6.823 + 0.075 V'_A + 0.396 V'_B \quad (6)$$

$$EEr = 49.293 + 0.878 V'_A + 29.592 V'_B \quad (7)$$

$$Re_v = 28.578 + 16.358 V'_A + 15.339 V'_B \quad (8)$$

$$Re_u = 11.223 + 6.424 V'_A + 6.023 V'_B \quad (9)$$

## Results and Discussion

### The concept of the Tesla valve

A Tesla valve, also known as a valve conduit (**Figure 1**), is a passive

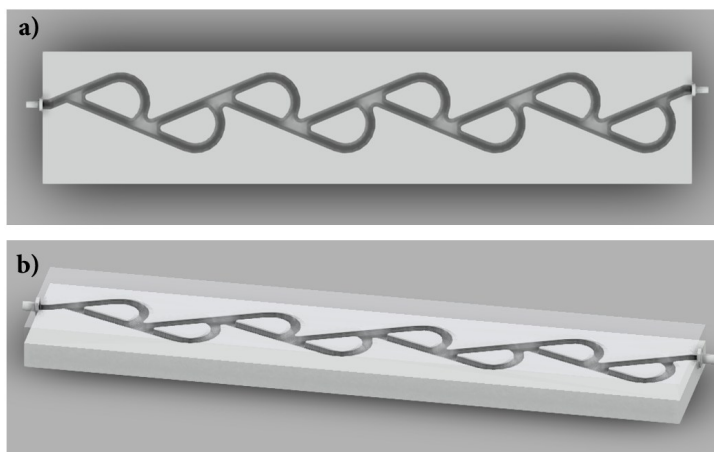


**Figure 1** | Reactor design: (a) top view; (b) side view.

The parameters shown in **Table 2** play a key role in the design and operation of the Tesla reactor, influencing its hydraulic properties and lifetime. The length of the reactor indicates a stretched structure, while the width and thickness are significant both for integration into hydraulic systems and for the mechanical strength of the overall structure. The volume of the used reactor, at 2.50 mL, indicates its compactness, which can be important in applications where system size has to be minimized. The flow diameter of the reactor is also a parameter that influences its performance, with a value of 0.25 cm indicating microfluidic operation, where viscous effects and capillary forces play a crucial role. The significant flow length, in turn, suggests an extended flow path, which is characteristic of design designed to increase hydraulic resistance in one direction while minimizing it in the opposite direction. The small flow cross-sectional area of 0.049 cm<sup>2</sup> limits the space for fluid transport, further enhancing the directional selectivity effect of

non-return valve with a fixed geometry that enables preferential fluid flow in one direction without the need for moving parts. The patent application describes the invention as a conduit with an interior featuring recesses, protrusions, or baffles that impose minimal resistance to fluid flow in the intended direction—aside from surface friction—while creating an almost impassable barrier to flow in the opposite direction. The absence of moving parts significantly enhances the valve's durability, particularly in applications subject to frequent pressure fluctuations [16].

the reactor. The combination of all geometric parameters determines the properties of the Tesla reactor, allowing it to function as a passive check valve [17].

### Reynolds number – how flow affect its value

To characterize the operation of the Tesla reactor, it is crucial to determine the Reynolds number and the apparent Reynolds number. This parameter is essential in chemical engineering as it allows for identifying the nature of fluid flow. Through hydrodynamic calculations, the volumetric flow rate ( $V$ ), the averaged flow rate ( $v$ ), and the apparent flow rate ( $u$ ) were determined, enabling the calculation of the Reynolds number and the apparent Reynolds number. This approach allows for establishing the correlation between the Reynolds number and the flow rate of the reactant streams, with the results presented in **Table 3**.

**Table 2** | Dimensions of Tesla valve reactor.

Parameter	Value
Length (mm)	196.50
Width (mm)	40.00
Thickness (mm)	8.50
Volume (mL)	2.50
Flow diameter (cm)	0.25
Flow length (cm)	50.93
Flow surface area (cm <sup>2</sup> )	0.049
Spigot outer diameter (mm)	4.00
Spigot inside diameter (mm)	1.80
T-piece outside diameter (mm)	5.00
Tee inside diameter (mm)	1.80

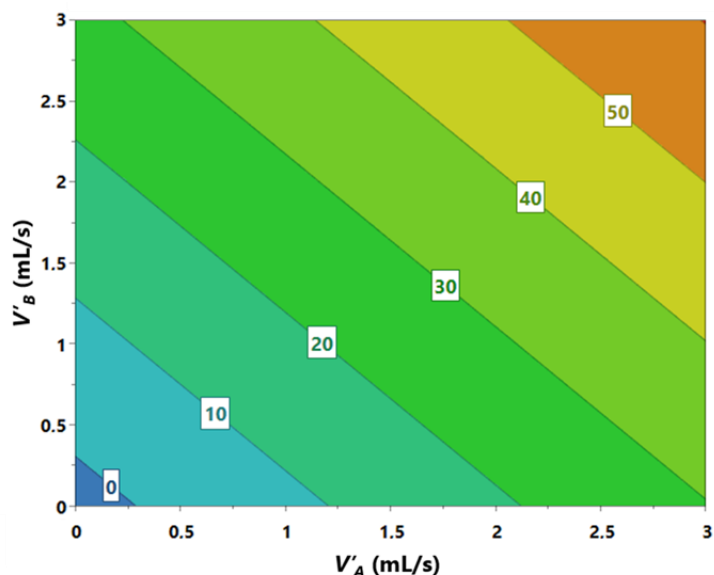
**Table 3** | Summary of calculation results for the model reaction of sodium hydroxide with hydrochloric acid.

Experiment number	$V'$ (mL/s)	$v$ (m/s)	$u$ (m/s)	$Re_v$ (-)	$Re_u$ (-)
1	0.015	0.00312	0.00123	8.741	3.433
2	0.015	0.00296	0.00116	8.284	3.253
3	0.033	0.00679	0.00267	18.998	7.460
4	0.052	0.01061	0.00417	29.684	11.657
5	0.048	0.00979	0.00385	27.400	10.760
6	0.060	0.01213	0.00476	33.924	13.322
7	0.061	0.01242	0.00488	34.752	13.647
8	0.074	0.01498	0.00588	41.906	16.457
9	0.093	0.01886	0.00741	52.771	20.723
10	0.081	0.01643	0.00645	45.962	18.049
11	0.114	0.02315	0.00909	64.764	25.433

The obtained values indicate that both Reynolds numbers depend on the flow rates of streams A and B. Both the average Reynolds number ( $Re_v$ ) and the apparent Reynolds number ( $Re_u$ ) increase with the rise in the volumetric flow rate. For example, for  $V' = 0.015$  mL/s, the values of  $Re_v$  and  $Re_u$  are 8.741 and 3.433, respectively, whereas for  $V' = 0.114$  mL/s, these values increase to 64.764 and 25.433, reaching their maximum values. In all conducted experiments, the values of  $Re_v$  and  $Re_u$  remain significantly below the transitional flow threshold ( $Re < 2100$ ). These values suggest laminar flow, resulting from the application of relatively low flow velocities. The values of the average Reynolds number are higher than those of the apparent Reynolds number for each analyzed case. This suggests that the average Reynolds number better describes the overall flow characteristics, while the apparent Reynolds number is more sensitive to local variations in flow

parameters. **Figures 2 and 3** show the dependence of the average and apparent Reynolds numbers, respectively, on the flow rates of the acid and hydroxide streams. The graphs indicate that the values of  $Re_v$  and  $Re_u$  increase as  $V'$  increases. For both parameters, the dependence on  $V'$  is almost linear, suggesting no sudden changes in the flow characteristics.

The graphs clearly demonstrate that within the examined range, the flow remains laminar, and further increases in flow rate could lead to transitional or turbulent flow. Esterl *et al.*, examined the influence of velocity flow on the catalytic process [18]. Their research was conducted in a different reactor than the Tesla reactor, but they observed the same correlation – the Reynolds number depends on the stream flow rate. Changes in reactor inflow resulted in changes in the Reynolds number, and due to the low velocity, the flow remained laminar.

**Figure 2** | Graph of the dependence of the average Reynolds number on the volumetric flow rate of streams A and B.

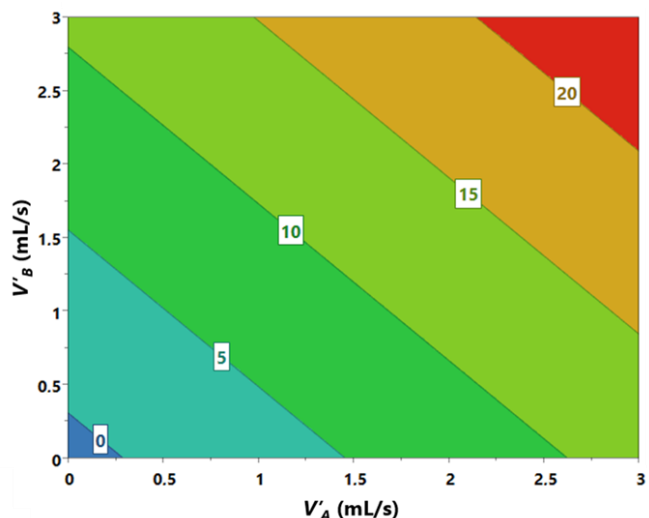


**Figure 3** | Graph of the dependence of the apparent Reynolds number on the volumetric flow rate of streams A and B.

#### Model reaction – how flow affect pH and absorbance

To determine the effect of the flow rate of the reactant streams on the pH of the samples obtained on  $t$ , the pH of the samples after leaving the reactor was measured at 0, 5 and 10 min of the process. The results of the measurements are gathered in **Table 4**.

The measurements showed that the pH of the obtained solutions is dependent on the flow rate of the individual streams. A high flow rate of the acid stream causes a shift in the pH value towards an acidic environment, while increasing the ratio of sodium hydroxide flow rate to acid raised the pH of the final solution. However, such changes were observed for experiments with high flow rates whereas for the other experiments, the pH of the solutions remained within the range of a neutral environment. The effect of the flow rate of each stream on the pH of the samples obtained was also analyzed. From **Figure 4** it can be observed that the pH of the samples tested depends mainly on the velocity of stream A,

increasing as the flow rate of the hydroxide increases. In contrast, the effect of the acid stream flow rate on the change in pH of the final solutions was less pronounced.

#### EE2 removal – how flow affect process duration and removal of estrogens

A key aspect of the research was testing the Tesla reactor in the process of estrogen degradation. Due to its design, the reactor ensures effective mixing of reagents, which enhances the degradation efficiency. Examining the impact of flow parameters on  $17\alpha$ -ethynylestradiol (EE2) degradation efficiency enables process optimization and assessment of the technology's potential under real-world conditions. The study analyzed the effect of reagent stream flow rates on the duration and efficiency of EE2 degradation. Stream A consisted of an EE2 solution, while stream B contained the laccase enzyme. The flow rates of both streams were

**Table 4** | Measured pH values of samples as a function of stream flow rate.

Experiment number	Stream flow rate A (mL/min)	Stream flow rate B (mL/min)	Measured pH		
			$t = 0$ (min)	$t = 5$ (min)	$t = 10$ (min)
1	0	1	8		
2	1	0	4.5		
3	1	1	7	7	7
4	1	2	7	7	6.5
5	2	1	7	7	7
6	2	2	7	7	7
7	1	3	6.5	6.5	6.5
8	3	1	7.5	7	7.5
9	2	3	7.5	6.5	7.5
10	3	2	7.5	7.5	7.5
11	3	3	6.5	7	7

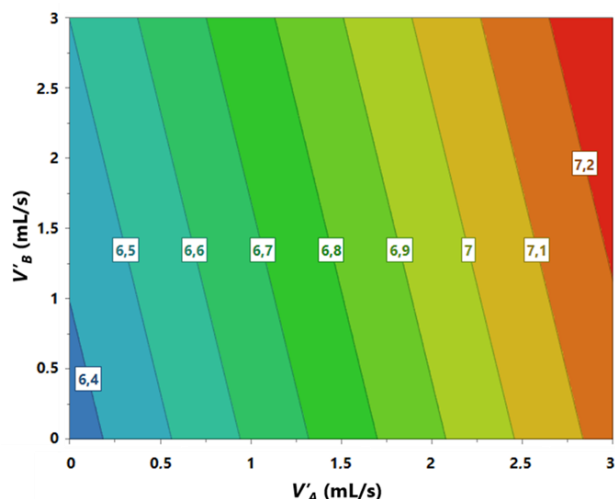


**Figure 4** | Graph of the pH dependence of samples on the flow velocity of streams A and B.

varied from 1 mL/min to 3 mL/min, enabling the evaluation of the relationship between these parameters and the effectiveness of estrogen degradation (**Figure 5**).

The graph shows that as the laccase flow rate increases, the degradation efficiency of EE2 rises, reaching a maximum of 84% when the laccase flow rate is three times higher than that of EE2. This indicates that a greater enzyme-to-substrate availability promotes more effective degradation. In contrast, the lowest EE2 removal efficiency, recorded at 38%, was observed when the

opposite flow rate ratio was applied (**Table 5**). These results are consistent with previous studies by Lloret *et al.*, in which, at a high EE2 concentration (4 mg/L) in an enzymatic membrane reactor and under conditions of reduced laccase activity, a removal efficiency of 85% was achieved.

Moreover, no biocatalyst inactivation was observed over 100 hours of operation, and estrogenicity was reduced by 84% [19]. For comparison, in the study conducted by Diório *et al.*, a photocatalytic membrane reactor (UV/H<sub>2</sub>O<sub>2</sub>/TiO<sub>2</sub>) was used,

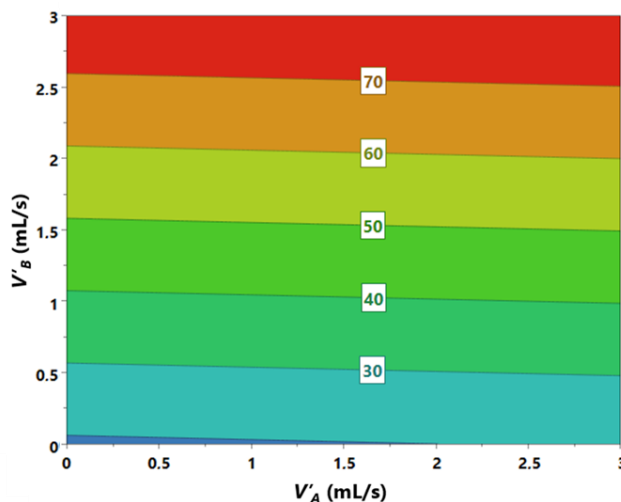


**Figure 5** | Graph of the dependence of the estrogen degradation efficiency on the velocity of the reactant streams.

achieving a maximum EE2 degradation rate of 2.9  $\mu\text{M}/\text{min}$  after 7 minutes of operation under optimized conditions (optimal H<sub>2</sub>O<sub>2</sub> concentration and pH). These findings confirm the high effectiveness of alternative strategies for micropollutant degradation; however, they require more complex operational conditions, such as UVC irradiation and the use of a heterogeneous catalyst [20].

In the last two experiments, degradation efficiency began to decline at high flow rates. This is likely due to the process duration being too short, leading to insufficient contact between the enzyme and estrogen. The research results indicate that both the flow rate of the streams and the process duration influence the efficiency of

enzymatic estrogen degradation. The degradation time of estrogens depends on the flow rate of both streams. At a flow rate of 1 mL/min, the degradation process lasted 163 and 172 seconds, respectively. A sixfold increase in flow rate reduced reaction duration by over eight times (from 163 seconds to 22 seconds), likely limiting enzyme-substrate interactions and resulting in lower degradation efficiency at higher flow rates.

Furthermore, degradation efficiency analysis shows that the Tesla reactor enables high-efficiency reactions, forming the basis for further research on the apparatus. The Tesla valve not only has potential for EE2 degradation but also for other compounds. As stated in the work of Li *et al.*, the Tesla valve significantly enhances

**Table 5** | Summary of the results of the studies on the enzymatic degradation of 17 $\alpha$ -ethynylestradiol.

Experiment number	Stream flow rate A (mL/s)	Stream flow rate B (mL/s)	EE2 removal efficiency (%)
1	0	1	0
2	1	0	0
3	1	1	75
4	1	2	79
5	2	1	61
6	2	2	76
7	1	3	84
8	3	1	38
9	2	3	73
10	3	2	49
11	3	3	58

the degradation rate of VOCs by a photocatalyst [21]. This system enables faster elimination of compounds such as toluene and formaldehyde. During the experiment, 97% degradation of toluene was achieved within 130 minutes and of formaldehyde within 175 minutes. These results are repeatable within a temperature range of 10 °C to 30 °C, indicating the stability of the system under various conditions. Such an application of the Tesla valve could serve as a foundation for developing modern purification methods that effectively remove unwanted compounds and minimize their negative impact on the environment.

### Concluding remarks

All obtained results confirm that an enzymatic reaction for the degradation of organic contaminants can be efficiently carried out in a reactor based on the Tesla valve structure. The study demonstrated that reaction efficiency primarily depends on the flow rate of the laccase stream through the reactor, with the highest degradation rate of 17 $\alpha$ -ethynylestradiol, reaching 84%, achieved when the enzyme flow rate was three times higher than that of the estrogen. It was also observed that high flow rates of both streams negatively affected the efficiency of laccase, which was attributed to an excessively short reaction and contact time. Hydrodynamic calculations further allowed for the determination of the flow type within the reactor showing the maximum recorded values were 64.764 for the averaged Reynolds number and 25.433 for the apparent Reynolds number, indicating that the system remained in the laminar regime. Additionally, an analysis of the relationship between pH and flow rate revealed that a high flow rate ratio of acid to hydroxide led to a shift in pH towards the acidic range, whereas the opposite scenario resulted in an alkaline pH. However, such phenomena were only observed at high flow rates, while in all other cases, the pH of the samples remained at 7. All obtained results provide a foundation for further studies on systems utilizing this type of apparatus, as its industrial application could offer significant economic benefits. The absence of moving parts that could wear out or fail, the elimination of the need for mechanical stirrers, the

simplicity of fabrication, and the backflow-preventing design—particularly crucial for low flow rates—would undoubtedly contribute to reducing the operational costs of the reactor in industrial settings. Furthermore, the practical implications of these findings are substantial. The reactor's simple construction and ease of manufacturing via 3D printing not only streamline the production process but also allow for rapid prototyping and adaptation to various industrial requirements. This versatility makes the Tesla valve reactor a promising candidate for large-scale applications in chemical and biotechnological industries, especially in wastewater treatment and pollutant removal processes where cost efficiency and reliability are paramount. The demonstrated balance between reaction efficiency and operational cost underlines the potential of this technology to revolutionize industrial practices in the field of enzymatic degradation.

### Acknowledgements

This work was supported by National Science Center Poland, as research project no. DEC 021/43/B/ST8/01854. This work also was supported by the Ministry of Science and Higher Education, Poland through a subsidy to Poznan University of Technology, research number 0912/SBAD/2511.

### References

- [1] Reisenbauer, J. C., Sicinski, K. M., & Arnold, F. H. (2024). Catalyzing the future: Recent advances in chemical synthesis using enzymes. *Current Opinion in Chemical Biology*, 83, 102536.
- [2] Cárdenas-Moreno, Y., González-Bacero, J., García Arellano, H., & del Monte-Martínez, A. (2023). Oxidoreductase enzymes: Characteristics, applications, and challenges as a biocatalyst. *Biotechnology and Applied Biochemistry*, 70, 2108–2135.
- [3] Mojto, M., Horváthová, M., Kiš, K., Furka, M., & Bakošová, M.

- (2021). Predictive control of a cascade of biochemical reactors. *Acta Chimica Slovaca*, 14(1), 51–59.
- [4] De Santis, P., Meyer, L.-E., & Kara, S. (2020). The rise of continuous flow biocatalysis – fundamentals, very recent developments and future perspectives. *Reaction Chemistry and Engineering*, 5(12), 2155–2184.
- [5] Katoh, S., Horiuchi, J.-i., & Yoshida, F. (2015). *Biochemical Engineering*. Wiley-VCH Verlag GmbH & Co. KGaA, Boschstr. 12, 69469 Weinheim, Germany.
- [6] Poppe, J. K., Fernandez-Lafuente, R., Rodrigues, R. C., & Ayub, M. A. Z. (2015). Enzymatic reactors for biodiesel synthesis: Present status and future prospects. *Biotechnology Advances*, 33(5), 511–525.
- [7] Grubecki, I. (2010). Optimal temperature control in a batch bioreactor with parallel deactivation of enzyme. *Journal of Process Control*, 20(5), 573–584.
- [8] Aziz, N. (2002). Optimal operation policies in batch reactors. *Chemical Engineering Journal*, 85(2-3), 313–325.
- [9] Hajba, L., & Guttman, A. (2016). Continuous-flow biochemical reactors: Biocatalysis, bioconversion, and bioanalytical applications utilizing immobilized microfluidic enzyme reactors. *Journal of Flow Chemistry*, 6(1), 8–12.
- [10] Britton, J., Majumdar, S., & Weiss, G. A. (2018). Continuous flow biocatalysis. *Chemical Society Reviews*, 47(15), 5891–5918.
- [11] Sitanggang, A. B., Drews, A., & Kraume, M. (2021). Enzymatic membrane reactors: Designs, applications, limitations and outlook. *Chemical Engineering and Processing - Process Intensification*, 108729.
- [12] Algieri, C., Coppola, G., Mukherjee, D., Shammas, M. I., Calabro, V., Curcio, S., & Chakraborty, S. (2021). Catalytic Membrane Reactors: The Industrial Applications Perspective. *Journal of Catalysis*, 11(6), 691.
- [13] Ching, C. B., & Chu, K. H. (1988). Modelling of a fixed bed and a fluidized bed immobilized enzyme reactor. *Applied Microbiology and Biotechnology*, 29(4), 316–322.
- [14] Bódalo, A., Gómez, J. L., Gómez, E., Bastida, J., & Máximo, M. F. (1995). Fluidized bed reactors operating with immobilized enzyme systems: Design model and its experimental verification. *Enzyme and Microbial Technology*, 17(10), 915–922.
- [15] Fidalgo, W. R. R., Ceron, A., Freitas, L., Santos, J. C., & Castro, H. F. (2016). A fluidized bed reactor as an approach to enzymatic biodiesel production in a process with simultaneous glycerol removal. *Journal of Industrial and Engineering Chemistry*, 38, 217–223.
- [16] Patent #: US001329559. United States Patent and Trademark Office. Office of the Chief Communications Officer, 2017.
- [17] Mohammadzadeh, K., Kolahdouz, E. M., Shirani, E., & Shafii, M. B. (2013). Numerical study on the performance of Tesla type microvalve in a valveless micropump in the range of low frequencies. *Journal of Micro-Bio Robotics*, 8(3-4), 145–159.
- [18] Esterl, S., Özmütlu, Ö., Hartmann, C., & Delgado, A. (2003). Three-dimensional numerical approach to investigate the substrate transport and conversion in an immobilized enzyme reactor. *Journal of Biotechnology and Bioengineering*, 83(7), 780–789.
- [19] Lloret, L., Eibes, G., Moreira, M. T., Feijoo, G., & Lema, J. M. (2013). Removal of Estrogenic Compounds from Filtered Secondary Wastewater Effluent in a Continuous Enzymatic Membrane Reactor. Identification of Biotransformation Products. *Environmental Science & Technology*, 47(9), 4536–4543.
- [20] Diório, A., Bergamasco, R., & Vieira, M. F. (2024). Performance of tube-in-tube membrane microreactor in E2/EE2 degradation via UV/H<sub>2</sub>O<sub>2</sub>/TiO<sub>2</sub> process. *Desalination and Water Treatment*, 100852.
- [21] Li, X., Cao, L. N. Y., Zhang, T., Fang, R., Ren, Y., Chen, X., Bian, Z., & Li, H. (2024). Optimizing photocatalytic performance in an electrostatic-photocatalytic air purification system through integration of triboelectric nanogenerator and Tesla valve. *Nano Energy*, 128, 109965.